



Published in final edited form as:

Pediatr Blood Cancer. 2009 August ; 53(2): 136–144. doi:10.1002/pbc.21968.

Bortezomib Reverses a Post-Translational Mechanism of Tumorigenesis for *Patched1* Haploinsufficiency in Medulloblastoma

Eri Taniguchi, PhD¹, Min Jung Cho, MD¹, Benjamin R. Arenkiel, PhD², Mark S. Hansen², Omar J. Rivera, PhD¹, Amanda T. McCleish¹, Stephen J. Qualman, MD³, Denis C. Guttridge, PhD⁴, Matthew P. Scott, PhD⁵, Mario R. Capecchi, PhD², and Charles Keller, MD^{1,*}

¹Greehey Children's Cancer Research Institute, Departments of Cellular & Structural Biology and Pediatrics, University of Texas Health Science Center, San Antonio, TX 78229 USA

²Howard Hughes Medical Institute and Department of Human Genetics, University of Utah, Salt Lake City, UT 84112 USA

³Children's Research Institute, Department of Laboratory Medicine, Columbus Children's Hospital, Columbus, OH 43205 USA

⁴Human Cancer Genetics Program, The Ohio State University College of Medicine, Columbus, OH 43210 USA

⁵Howard Hughes Medical Institute and Departments of Developmental Biology, Genetics, and Bioengineering, Stanford University School of Medicine, Stanford, California 94305 USA

Abstract

Background—Tumor initiation has been attributed to haploinsufficiency at a single locus for a large number of cancers. *Patched1* (*Ptc1*) was one of the first such loci, and *Ptc1* haploinsufficiency has been asserted to lead to medulloblastoma and rhabdomyosarcoma in mice.

Procedure—To study the role of *Ptc1* in cerebellar tumor development and to create a preclinical therapeutic platform, we have generated a conditional *Ptc1* haploinsufficiency model of medulloblastoma by inactivating *Ptc1* in *Pax7*-expressing cells of the cerebellum.

Results—These mice developed exclusively medulloblastoma. We show that despite the presence of transcription of *Ptc1*, *Ptc1* protein is nearly undetectable or absent in tumors. Our results suggest that *Ptc1* loss of function is complete, but achieved at the protein level rather than by the classic genetic two-hit mechanism or a strict half-dosage genetic haploinsufficiency mechanism. Furthermore, we found that bortezomib, a 26S proteasome inhibitor, had a significant anti-tumor activity *in vitro* and *in vivo*, which was accompanied by restoration of *Ptc1* protein and downregulation of the hedgehog signaling pathway. The same effect was seen for both human and mouse medulloblastoma tumor cell growth.

Conclusions—These results suggest that proteasome inhibition is a potential new therapeutic approach in medulloblastoma.

Keywords

Medulloblastoma; Haploinsufficiency; Hedgehog; Patched1; Proteasome; Bortezomib

*Corresponding author: Greehey Children's Cancer Research Institute, University of Texas Health Science Center, 8403 Floyd Curl Drive, MC-7784, San Antonio, TX 78229-3900 USA, Tel: (210)562-9062, Fax: (210)562-9014, kellerc2@uthscsa.edu.

Introduction

The two hit hypothesis proposed that loss of both copies of a tumor suppressor gene could be required for tumor initiation [1]. However, in developmental biology [2] and cancer biology [3] haploinsufficiency has been recognized as a mechanism by which altered gene dosage can lead to stochastic imbalances in gene expression with phenotypic or tumorigenic consequences. A multitude of cancers have been attributed to haploinsufficiency of any one of nearly 2 dozen genes [3].

One of the first loci to be studied with respect to haploinsufficiency was the *Patched1* (*Ptc1*) gene. *Ptc1* encodes a 12-transmembrane-domain protein that serves as a receptor for Hedgehog signaling proteins, and haploinsufficiency of *Ptc1* has been suggested to lead to primitive neuroectodermal tumor of the cerebellum (medulloblastoma) and rhabdomyosarcoma in mice (4–6). However, this assertion has been debated, with seven papers from five groups on both sides of the issue. Using differing techniques, each group has reported that *Ptc1* is, or is not, transcribed from the wild-type allele in medulloblastomas that arise in *Ptc1* heterozygous mice [4–10]. Further complicating the issue, recent data suggest that *Ptc1* is alternatively spliced, having at least four alternative first exons [11,12]. The splice variants may have specific biological significance because each isoform has a different stability and different susceptibility to proteasome-mediated degradation *in vitro* [13] and possibly *in vivo*.

To study the role of *Ptc1* in cerebellar tumor development, we have generated a novel conditional *Ptc1* model of tumorigenesis by Cre/Lox inactivation of a single conditional *Ptc1* allele using a *Pax7-Cre* knock-in. Although *Pax7* is expressed in both the developing cerebellum and muscle satellite cells [14], our mice developed exclusively medulloblastomas (and not rhabdomyosarcomas). In this report we directly compare splice variation in our conditional medulloblastoma model to existing germline models. We have uncovered that *Ptc1* in mice and humans is significantly regulated at the post-translational rather than simply at the transcriptional level. Our results suggest that inhibiting the 26S proteasome can not only restore *Ptc1* signaling imbalance in medulloblastoma tumor cells but can also serve as a potential new therapeutic approach.

Methods

Genomic Clones Isolation

Genomic DNA clones were isolated from a Lambda bacteriophage library of mouse strain SvJ-129 (Stratagene, La Jolla, CA) following the manufacturer's guidelines. We identified a 9 kb clone spanning the intron between exons 1C and 1B to intron 2 of *Ptc1*, and a 6.5 kb clone spanning the intron between exons 1A and 2 to intron 2 of *Ptc1*.

Targeted Mouse Line Production

All animal studies were conducted under an institutional IACUC-approved protocol. For the *Ptc1* conditional knock-out mouse line, a targeting vector was constructed for which Lox511 sites flank exons 1B, 1, 1A and 2 of the *Ptc1* gene. This targeting vector was electroporated into R1 embryonic stem cells subjected to positive and negative selection [15]. A total of 144 colonies were analyzed by Southern hybridization using Sall/SpeI restriction enzyme digestion of genomic DNA and a 1.5kB XhoI-XhoI 5' external probe. 17 clones were identified with a targeted modification of the *Ptc1* locus. Cells from one of these recombinant clones were microinjected into C57BL/6 blastocysts to generate chimeric mice. Chimeric mice were mated to C57BL/6 females, and their Agouti offspring were tested by Southern hybridization to confirm germline transmission of the *Ptc1*^{F1-2p} conditional allele. The FRT-flanked *neomycin resistance gene* (*Neo*) was removed by breeding *Ptc1*^{F1-2p/wt}

mice to transgenic mice expressing *Flp-e* [16], thereby generating *Ptc1^{F1-2m/wt}* mice. Generation of the *Pax7^{ICNm/WT}* mice was previously described [17]. Genotyping of mouse lines is detailed in Supplemental Methods.

Treatment with bortezomib in vitro and in vivo

Medulloblastoma cell lines were plated in 60 mm dish (at 1×10^5 cells per dish) and cultured overnight. The cells were treated at the indicated concentration of bortezomib/PS-341 (Velcade[®], Millennium Pharmaceutical, Cambridge, MA) or 0.05 % DMSO (control). Cells were incubated for an additional 24 hours and harvested for RNA and protein isolation. For *in vitro* growth inhibition assay, medulloblastoma cell lines were plated in 96-well plates (5×10^3 cells per well) and cultured for overnight. The cells were treated with different concentrations of bortezomib/DMSO (0–1 μ M) or 0.5 % DMSO (control). Cells (duplicate samples for each concentration) were then incubated for an additional 72 hours, followed with CellTiter-Glo[®] Luminescent Cell Viability Assay (Promega, Madison, WI). For *in vivo* effect of bortezomib, medulloblastoma mice at early symptom or wildtype mice at two months old were treated with bortezomib (1 mg/kg) by intraperitoneal injection once weekly. Mice were sacrificed after two doses and cerebellums were processed for immunoblotting, quantitative RT-PCR.

Immunoprecipitation and Immunoblotting

For *Ptc1* immunoblotting of medulloblastoma cell lines, cells were lysed in RIPA buffer containing a phosphatase inhibitor and a Tyr/Ser-Thr protease inhibitor (Sigma-Aldrich, St. Louis, MO) and centrifuged at $20,000 \times g$ for 15 min. Endogenous *Ptc1* was immunoprecipitated with Rabbit polyclonal *Ptc1* antibody (sc-9016; Santa Cruz, CA) coupled to protein A-Sepharose (GE Healthcare Bio-Sciences Corp., Piscataway, NJ). The immunoprecipitates were further washed with RIPA buffer and subjected to immunoblotting as described below. Tumor tissues were lysed in RIPA buffer containing a phosphatase inhibitor and a protease inhibitor. For *Ptc1* immunoblotting of tumor tissues, the lysates were homogenized using a non-foaming homogenizer generator for 20 seconds twice and centrifuged at 8,000g for 20 minutes. The resulting supernatants were taken for immunoblot analysis. Rabbit polyclonal *Ptc1* antibody (sc-9016; Santa Cruz, CA), rabbit polyclonal *Gli1* antibody (sc-20687), and rabbit polyclonal *Shh* antibody (sc-9024) were used at a concentration of 1:200 while monoclonal β -actin antibody (Developmental Studies Hybridoma Bank, University of Iowa) was used at 1:500. Appropriate horseradish peroxidase-conjugated secondary antibodies (Vectorlabs, Burlingame, CA) were used at 1:4000 and chemiluminescence was detected using Western Pico substrate (Pierce Biotechnology, Rockford, IL).

Other Experimental Methods

Additional detailed methods for *Histology and Immunohistochemistry*, *RNA Isolation and RT-PCR*, and *Culture of Medulloblastoma Cell Lines* are given in Supplemental Methods.

Results

Design and generation of targeted mouse lines

The *Ptc1^{F1-2m}* conditional allele was designed to express wild-type *Ptc1* until excision by Cre whereupon *Lox511*-flanked exons 1B, 1, 1A, and 2 are removed to inactivate the *Ptc1* gene (Fig. 1A). In this report we use the original nomenclature for *Ptc1* splice variants described by Shimokawa *et al* [18], noting that other nomenclatures have been proposed [12]. Following electroporation, 19 of 144 candidate embryonic stem cell clones were heterozygous for the targeted mutation by Southern hybridization (Fig. 1B). Germline

transgenic mice were established that carried the *floxed* targeting vector. The *Neo* selection cassette was removed by Flpe-mediated recombination to generate viable and fertile *Ptc1^{F1-2m/WT}* heterozygous mice. These mice were followed for greater than 15 months and did not develop cancers in the absence of an accompanying Cre allele.

A second mouse line directing Cre expression to the cerebellum, *Pax7^{ICNm}*, has been previously described [17]. In brief, an *IRES-Cre* cassette was targeted to the 3' untranslated region of the *Pax7* gene between the stop codon and the polyadenylation signal to allow expression of *Cre* as a second cistron of the *Pax7* mRNA, without interfering with native *cis*-elements. These mice have no overt cerebellar or musculoskeletal phenotype. Cre expression in developing spinal cord and myogenic lineages has been previously shown [17]. In this study, we examined the fate of *Pax7*-expressing cells contributing to the developing brain using an *eYFP* reporter mouse line, *Rosa26^{tm1(EYFP)Cos}* [19]. In neonatal *Pax7^{ICNm/WT} Rosa26^{tm1(EYFP)Cos/WT}* mice, the primordial cerebellum and midbrain were found to be derived from the *Pax7* lineage (Fig. 1C–D).

Pax7-targeted heterozygosity of *Ptc1* leads to medulloblastoma

To induce *Ptc1* haploinsufficiency in the *Pax7*-expressing cells, we crossed sires carrying the *Pax7^{ICNm}* allele with dams carrying the *Ptc1* conditional allele, *Ptc1^{F1-2m}*. The resulting doubly heterozygous offspring, *Pax7^{ICNm/WT} Ptc1^{F1-2m/WT}*, were viable and fertile and did not have gross morphological abnormalities. Although no tumors were noted in 225 *Ptc1^{F1-2m/WT}* singly heterozygous animals followed for up to 500 days, 9 out of 30 doubly heterozygous *Pax7^{ICNm/WT} Ptc1^{F1-2m/WT}* animals were ataxic with an initial onset of 88–100 days (Fig. 2A). These animals had developed rapidly-growing tumors of the cerebellum (Fig. 2B). Tumor cells had a high nuclear:cytoplasmic ratio (Fig. 1E), and were immunopositive for β 3-Tubulin, NeuN, and synaptophysin (Fig. 1D–F). The tumors, consistent with classic-histology medulloblastoma, all invaded the subarachnoid space (data not shown). In addition, 4 out of 9 tumor-bearing animals had evidence of gross or microscopic leptomeningeal metastasis (Fig. 1G–H). Lineage tracing suggests that the cell of origin of these tumors is the external granular layer neuronal precursor (Supplemental Figures 1 and 2).

Mutations in *p53* increase the penetrance and accelerate the onset of medulloblastoma in *Pax7^{ICNm/WT} Ptc1^{F1-2m/WT}* mice

Previous reports have shown that *p53* heterozygosity or homozygosity accelerates the onset and increases the frequency of medulloblastoma in mice heterozygous for *Ptc1* [20]. The higher penetrance of tumors in *Ptc1-p53* mice (*Ptc1^{tmMPS/WT} p53^{del/del}*) make this compound germline model very useful for preclinical therapeutic experiments. However, the rapid onset of disease in the first 1–3 months of life might make maintenance of a breeding colony problematic.

We sought to improve upon the existing compound germline *Ptc1-p53* model by creating a compound conditional model whose parental breeding lines would be less cancer-prone. For these studies we introduced a *p53* conditional allele, *p53^{F2-10/WT}* [21] into our model. Symptomatic tumor onset was significantly reduced from 90 – 100 days for *Pax7^{ICNm/WT} Ptc1^{F1-2m/WT}* mice to as early as 32– 65 days for *Pax7^{ICNm/WT} Ptc1^{F1-2m/WT} p53^{F2-10/WT or F2-10}* mice (Supplemental Fig. 3). No change in histology was noted, and tumors maintained classic medulloblastoma histology as well as signs of rapid cell turnover such as frequent tingible body macrophages and mitotic Figs (Supplemental Fig. 3).

Messenger RNA Splice variants of *Ptc1* are expressed in medulloblastomas

Ptc1 has been reported to have several first exons -1, -1A, -1B and 1C (Supplemental Fig. 4A–B). In cell culture experiments, exon 1B and 1C are upregulated in cells that have received a Hedgehog signal while exon 1 and exon 1A are not upregulated by Hedgehog [13]. In our conditional model as well as the germline *Ptc1^{tmMPS}* model, exon 1, exon 1A and exon 1B are excised by Cre but exon 1C is not excised. Therefore, conveniently, the presence of exon -1, -1A, or -1B containing transcripts in tumor tissue from heterozygous animals would be indicative of expression from the normal copy of the *Ptc1* locus.

To investigate the expression of *Ptc1* splice variants in medulloblastoma, we performed quantitative RT-PCR in medulloblastomas derived from our conditional allele, *i.e.* *Ptc1^{F1-2m/WT}*, or from a well-studied germline model, *i.e.* *Ptc1^{tmMPS/WT}* [4,7,22]. As a control we used P9 cerebellums from wildtype mice or germline *Ptc1^{DELI-2/WT}* mice generated using our conditional *Ptc1* allele (described in Supplemental Results). Some medulloblastoma mice carried the conditional knock-out allele of *p53*. All medulloblastoma derived from the conditional and germline knockout mice of *Ptc1* expressed multiple splice variants of *Ptc1* (Fig. 3A). *Ptc1-1B* was consistently expressed in all tumors as well as wildtype cerebellums or preneoplastic *Ptc1^{DELI-2/WT}* cerebellums, while the *Ptc1-1* variant was variably present in the tumors, and *Ptc1-1A* was not present in any tumors or control samples. Since *Ptc1-1B* and *Ptc1-1* can be produced only from the wildtype allele, these results suggest that the wildtype allele of *Ptc1* is in fact transcriptionally active in these tumors, in agreement with certain previous reports [6–8].

In addition to the splice variants described above, we detected dominant expression of an alternative splice variant initiating at exon 1C that skipped exon 2 (referred as 1C³) in tumors, while an intact splice variant of exon 1C (referred as 1C-2-3) was present in wildtype cerebellums and preneoplastic *Ptc1^{DELI-2/WT}* cerebellums. *Ptc1-1C³* is assumed to be the same sequence as the previously characterized, naturally occurring variant PTCH1-1CΔE2 [13]. Functionally, the 1C³ splice variant would be expected to produce a protein similar to splice variants 1 or 1A, which initiates translation in exon 3 [13]. Furthermore, the presence of 1C-2-3 in control cerebellar samples, but not tumor samples, suggests that tumor samples were likely not contaminated with non-tumor tissues. Supporting this assertion, we performed RT-PCR for *Ptc1* splice variants in paired tumor samples and cell lines derived from the same tumor samples, as well as 8 weeks old cerebellums (Supplemental Fig. 5A). In every case for tumor and tumor cell lines, the wildtype *Ptc1* allele was found to actively transcribe its mRNA (*Ptc1-1B* and *Ptc1-1*).

Recently, a potentially biologically significant splice variant called *Ptc1-12b* was reported, which encodes a dominant negative isoform of Ptc1 [23]. In the case of our model, we did not detect *Ptc1-12b* expression in tumors with any of the genotypes that we tested (data not shown).

Ptc1 protein product is nearly undetectable or absent in these experimental models of medulloblastoma

To examine whether *Ptc1* splice variants generate corresponding proteins of varying size, we performed immunoblotting of P9 wildtype cerebellums and murine medulloblastomas using an anti-Ptc1 antibody made against its C-terminus (amino acids 1181–1447) (Fig. 3B). This C-terminal region is common to all reported splice variants of *Ptc1* and contains a conserved PPXY ubiquitin ligase binding motif that negatively regulates its stability [24]. In wildtype P9 cerebellums, only an approximately 145 kDa isoform was detected. The 145 kDa band was approximately the size predicted for certain *Ptc1* mRNA splice variants (Supplemental Fig. 4C). However, in tumors from conditionally deleted and germline-

knockout mice, no proteins were detected of the predicted molecular weights of isoforms 1B (160kDa), 1C (154 kDa), 1 or 1A (144 kDa) or 1C^{Δ3}/1C^{ΔE2} (also 144 kDa) – despite the presence of the *Ptc1* messenger RNAs. The functional absence of Ptc1 protein was also evident by examining downstream targets that Ptc1 inhibits: the expression of *Gli1* and *CyclinD2* was 100 – 1000 fold higher in tumors than P9 wildtype cerebellums (Fig. 3C) in medulloblastomas of all genotypes that we tested.

The proteasome-dependent degradation of Ptc1 may play an important role in development and progression of medulloblastoma

The presence of *Ptc1* mRNA transcripts but paucity of Ptc1 protein in medulloblastoma led us to consider mechanisms of post-translational regulation of Ptc1, such as the proteasome. To assess the effect of proteasome inhibition on Ptc1 protein stability, we utilized bortezomib/PS-341 to treat medulloblastoma-prone *Pax7^{ICNm}/WT Ptc1^{F1-2m}/WT p53^{F2-10/F2-10}* mice at the onset of disease (ataxia). Control cohorts included untreated tumor-bearing mice, untreated 2 month old wildtype mice, and 2 month old wildtype mice given the same dose of bortezomib as treated medulloblastoma mice. Compared to untreated tumor-bearing mice, treated tumor-bearing mice had significantly longer survival (10 days vs 1 days, $p=0.00036$) (Fig. 4A). We explored whether this effect might be at least partially attributable to Ptc1 protein restoration in tumors. By immunoblotting, bortezomib had no effect on the Ptc1 protein level from wildtype cerebellums. Surprisingly, however, the 145kDa Ptc1 protein was restored in bortezomib treated medulloblastomas *in vivo* (Fig. 4B). In order to demonstrate that Ptc1 protein was restored in the tumor cells and not contaminating cells from the stroma, and that bortezomib suppressed tumor cell growth, we moved to *in vitro* studies with medulloblastoma cell lines. Compared with the effect of bortezomib on several other tumor cell types [25–27], medulloblastoma cell lines showed high sensitivity by *in vitro* cell growth assay ($IC_{50} \leq 5nM$, Fig. 4C). At the RNA level, cell lines were confirmed to express *Ptc1* splice variants *Ptc1-1* and *Ptc1-1C^{Δ3}* (Supplemental Fig. 5), thus affirming that tumor cells (rather than stromal-derived cells) express *Ptc1* RNA. As bortezomib dose increased from 1nM to 10nM, the level of *Ptc1* transcripts also decreased, which would be expected if Ptc1 function was restored since negative autoregulation of this locus occurs [22,28]. At the protein level, Ptc1 protein increased substantially with escalating doses of bortezomib. At the same time, Ptc1 downstream targets *Gli1* and *CyclinD2* also decreased in a dose-dependent manner (Fig. 4D). Whereas bortezomib's classical mechanism of action is to block NF- κ B activation [26,29], we showed that although NF- κ B signaling is partially affected by bortezomib, inhibition of NF- κ B had little effect on medulloblastoma cell growth (Supplemental Results, Supplemental Fig. 6). These data suggest that Shh signaling pathway is dampened by restoration of Ptc1 as a result of bortezomib treatment, and that proteasome-dependent degradation of Ptc1 protein may play an important role in tumor maintenance and progression for medulloblastoma.

The effect of bortezomib on tumor cell growth and Ptc1 protein levels is seen in human as well as mouse medulloblastoma cells

To extend our findings that bortezomib dampens Shh signaling in not only mouse but also human medulloblastoma, an *in vitro* cell growth assay of bortezomib was performed in three human medulloblastoma cell lines (DAOY, D283 and D341). As shown in Fig. 5A, all cell lines showed high sensitivity to bortezomib ($IC_{50} \leq 10 nM$). To affirm that bortezomib led to inhibition of Shh signaling pathway, we compared the effect of bortezomib treatment to the effect of *Ptc1* transfection in human (DAOY) and mouse (U26137) medulloblastoma cell lines.

Whereas the level of Ptc1 was too low to detect in control cells (Fig. 5B), accumulation of Ptc1 protein was detected in bortezomib-treated cells at levels comparative to Ptc1

transfection for both cell lines. For human and mouse cells treated either with bortezomib or *Ptc1* transfection, the level of *Gli1* transcripts decreased, which suggests that Ptc1 function was restored and Shh signaling was dampened (Fig. 5C, left panel) [22,28]. As expected, treatment of bortezomib did not increase *Ptc1* transcripts, which itself is a Ptc1 downstream target. We did observe high level of *Ptc1* transcripts in transfected cells, which is attributable to *Ptc1* plasmid (Fig. 5C, right panel). To demonstrate whether dampening of Shh signaling was functionally relevant to tumor growth in human or mouse medulloblastoma, we performed dose-response growth assays with cyclopamine, a small molecule which functions similarly to Ptc1 by the inhibition of Smoothed [9]. Inhibition of growth was observed at an IC50 comparable to other studies of cyclopamine-sensitive tumors (Supplemental Fig. 7) [30,31]. Taken together, these data suggest that at least one mechanism of bortezomib in medulloblastoma (mouse or human) is to inhibit tumor cell growth by restoring Ptc1 and dampening Shh overdrive.

Discussion

In this report we present a novel conditional *Ptc1* mouse model of medulloblastoma. Tumors in our model are similar to the most common clinical presentation: classic histology, uniform local invasion, and frequent leptomeningeal metastasis. Our conditional model shares with existing germline *Ptc1* mouse models a strong interaction with *p53*. Homozygous loss of *p53* function increases tumor penetrance to 100% [20]. Our conditional model has the advantage that parental breeding lines are not themselves prone to dying of tumors before reaching breeding age, nor are the mice prone to non-CNS tumors. Therefore, our conditional model has certain advantages for preclinical therapeutic trials. Other conditional alleles of *Ptc1* have been published [32–34], and a different report of a conditional model of medulloblastoma recently underscored the power of these models for understanding tumor cell biology [35].

Haploinsufficiency of *Ptc1* has been suggested as a mechanism of tumor initiation in mice [8] and humans [36], although this assertion is controversial. Ptc1 is the receptor for Sonic hedgehog, and single allele (oncogenic) imbalances for other components of the Shh signaling pathway have been shown to lead to tumorigenesis [37]. Yet whether *Ptc1* tumorigenesis follows the classic two-hit mechanism or a haploinsufficiency mechanism remains strongly debated [4–10]. Using tumor samples from our conditional model as well as tumor samples from other germline knockout models [4,7], we demonstrate that multiple splice variants of *Ptc1* are produced in the previously published germline mouse model as well as our new conditional model. These results indicate retention of a wildtype allele competent to produce *Ptc1* mRNA transcripts. The absence of Ptc1 protein from all mouse tumor models examined suggests that loss of function of Ptc1 function is achieved at the protein level rather than by a classic genetic two-hit mechanism or a strict half-dosage genetic haploinsufficiency mechanism.

In an effort to overcome the post-translational downregulation of Ptc1 in medulloblastoma, we evaluated whether bortezomib/PS-341, a 26S proteasome inhibitor, could restore Ptc1 protein levels and function in human and mouse medulloblastoma cell lines. Our results show restoration of Ptc1 and transcriptional downregulation of sonic hedgehog targets *Gli1* and *CyclinD2* as a result of treatment of bortezomib *in vitro*, suggesting both that Shh signaling pathway is inhibited by restoration of Ptc1 and that proteasome-dependent degradation of Ptc1 is an unrecognized mechanism of haploinsufficiency-mediated tumorigenesis. Observations that tumor growth of mouse and human medulloblastoma can be inhibited by the Shh pathway inhibitors cyclopamine (Supplemental Fig. 7) and KAAD-cyclopamine [9] further strengthens the pathophysiological significance of Shh signaling in this disease.

Our results are consistent with emerging evidence suggesting that ubiquitin- and proteasome-mediated cleavage of Ptc1 may be rate-limiting to its function. Two recent reports indicate that the Ptc1 C-terminus contains a conserved PPXY ubiquitin ligase binding motif that negatively regulates Ptc1 stability [24], and that the stability of all Ptc1 isoforms was increased by a proteasome inhibitor, MG-132 [13]. We are careful to recognize that in our experiments, the anti-tumor effect of bortezomib *in vitro* and *in vivo* may have been mediated by parallel mechanisms synergistic or additive to Ptc1 restoration. Bortezomib is known to modulate a variety of signaling pathways not limited to Shh and NF- κ B but also c-Jun N-terminal kinase and p53 [38]; however, any major consequence of inhibiting the p65-mediated, classical NF- κ B signaling pathway was ruled out, as is any role of p53 upregulation because the preclinical model we studied inactivates both *p53* genes. Furthermore, bortezomib not only restored Ptc1 function to a level comparable to direct Ptc1 transfection, but also had a substantial anti-tumor effect on primary tumor cell cultures ($IC_{50} \leq 5nM$). Whether dampening Shh signaling is or is not the sole mechanism of bortezomib action does not take away from the fact that this proteasome inhibitor is an effective new agent for this disease. Given that bortezomib normally has limited CNS penetration [39] except where tumors may break down the blood-brain barrier, we are excited to consider the possibility that new proteasome or ubiquitin ligase inhibitors that more readily penetrate the blood brain barrier may soon be developed.

Supplementary Material

Refer to Web version on PubMed Central for supplementary material.

Acknowledgments

We thank the laboratory of Robert Wechsler-Reya at Duke University for providing germline *Ptc1* tumor samples; Tom Curran and Jessica Ng for supplying *Ptc1*^{+/-} and *Ptc1*^{+/-} *p53*^{-/-} tumor materials; Dan Fufts, Lyn Pedone, Andrea Rodriguez, Mary Blandford and Katherine Ladner for technical assistance; Dr. Roger McLendon for histological evaluation; The Pediatric Brain Tumor Foundation of the United States, The St. Baldrick's Foundation, The National Brain Tumor Society, The Cancer Therapy and Research Center (grant number P30CA54174) and the Huntsman Cancer Institute's Center for Children for grant support. The authors declare no conflicts of interest.

References

1. Knudson AG Jr. Mutation and cancer: statistical study of retinoblastoma. *Proc Natl Acad Sci U S A*. 1971; 68(4):820–823. [PubMed: 5279523]
2. Cook DL, Gerber AN, Tapscott SJ. Modeling stochastic gene expression: implications for haploinsufficiency. *Proc Natl Acad Sci U S A*. 1998; 95(26):15641–15646. [PubMed: 9861023]
3. Santarosa M, Ashworth A. Haploinsufficiency for tumour suppressor genes: when you don't need to go all the way. *Biochim Biophys Acta*. 2004; 1654(2):105–122. [PubMed: 15172699]
4. Oliver TG, Read TA, Kessler JD, et al. Loss of patched and disruption of granule cell development in a pre-neoplastic stage of medulloblastoma. *Development*. 2005; 132(10):2425–2439. [PubMed: 15843415]
5. Kim JY, Nelson AL, Algon SA, et al. Medulloblastoma tumorigenesis diverges from cerebellar granule cell differentiation in patched heterozygous mice. *Dev Biol*. 2003; 263(1):50–66. [PubMed: 14568546]
6. Romer JT, Kimura H, Magdaleno S, et al. Suppression of the Shh pathway using a small molecule inhibitor eliminates medulloblastoma in *Ptc1*^{+/-}*p53*^{-/-} mice. *Cancer Cell*. 2004; 6(3):229–240. [PubMed: 15380514]
7. Wetmore C, Eberhart DE, Curran T. The normal patched allele is expressed in medulloblastomas from mice with heterozygous germ-line mutation of patched. *Cancer Res*. 2000; 60(8):2239–2246. [PubMed: 10786690]
8. Zurawel RH, Allen C, Wechsler-Reya R, et al. Evidence that haploinsufficiency of *Ptch* leads to medulloblastoma in mice. *Genes Chromosomes Cancer*. 2000; 28(1):77–81. [PubMed: 10738305]

9. Berman DM, Karhadkar SS, Hallahan AR, et al. Medulloblastoma growth inhibition by hedgehog pathway blockade. *Science*. 2002; 297(5586):1559–1561. [PubMed: 12202832]
10. Uhmann A, Ferch U, Bauer R, et al. A model for PTCH1/Ptch1-associated tumors comprising mutational inactivation and gene silencing. *Int J Oncol*. 2005; 27(6):1567–1575. [PubMed: 16273213]
11. Kogerman P, Krause D, Rahnama F, et al. Alternative first exons of PTCH1 are differentially regulated in vivo and may confer different functions to the PTCH1 protein. *Oncogene*. 2002; 21(39):6007–6016. [PubMed: 12203113]
12. Nagao K, Toyoda M, Takeuchi-Inoue K, et al. Identification and characterization of multiple isoforms of a murine and human tumor suppressor, patched, having distinct first exons. *Genomics*. 2005; 85(4):462–471. [PubMed: 15780749]
13. Shimokawa T, Svard J, Heby-Henricson K, et al. Distinct roles of first exon variants of the tumor-suppressor Patched1 in Hedgehog signaling. *Oncogene*. 2007; 26(34):4889–4896. [PubMed: 17310997]
14. Oustanina S, Hause G, Braun T. Pax7 directs postnatal renewal and propagation of myogenic satellite cells but not their specification. *Embo J*. 2004; 23(16):3430–3439. [PubMed: 15282552]
15. Mansour SL, Thomas KR, Capecchi MR. Disruption of the proto-oncogene int-2 in mouse embryo-derived stem cells: a general strategy for targeting mutations to non-selectable genes. *Nature*. 1988; 336(6197):348–352. [PubMed: 3194019]
16. Rodriguez CI, Buchholz F, Galloway J, et al. High-efficiency deleter mice show that FLPe is an alternative to Cre-loxP [letter]. *Nat Genet*. 2000; 25(2):139–140. [PubMed: 10835623]
17. Keller C, Hansen MS, Coffin CM, et al. Pax3:Fkhr interferes with embryonic Pax3 and Pax7 function: implications for alveolar rhabdomyosarcoma cell of origin. *Genes Dev*. 2004; 18(21):2608–2613. [PubMed: 15520281]
18. Shimokawa T, Rahnama F, Zaphiropoulos PG. A novel first exon of the Patched1 gene is upregulated by Hedgehog signaling resulting in a protein with pathway inhibitory functions. *FEBS Lett*. 2004; 578(1–2):157–162. [PubMed: 15581634]
19. Srinivas S, Watanabe T, Lin CS, et al. Cre reporter strains produced by targeted insertion of EYFP and ECFP into the ROSA26 locus. *BMC Dev Biol*. 2001; 1:4. [PubMed: 11299042]
20. Wetmore C, Eberhart DE, Curran T. Loss of p53 but not ARF accelerates medulloblastoma in mice heterozygous for patched. *Cancer Res*. 2001; 61(2):513–516. [PubMed: 11212243]
21. Jonkers J, Meuwissen R, van der Gulden H, et al. Synergistic tumor suppressor activity of BRCA2 and p53 in a conditional mouse model for breast cancer. *Nat Genet*. 2001; 29(4):418–425. [PubMed: 11694875]
22. Goodrich LV, Milenkovic L, Higgins KM, et al. Altered neural cell fates and medulloblastoma in mouse patched mutants. *Science*. 1997; 277(5329):1109–1113. [PubMed: 9262482]
23. Uchikawa H, Toyoda M, Nagao K, et al. Brain- and heart-specific Patched-1 containing exon 12b is a dominant negative isoform and is expressed in medulloblastomas. *Biochem Biophys Res Commun*. 2006; 349(1):277–283. [PubMed: 16934747]
24. Lu X, Liu S, Kornberg TB. The C-terminal tail of the Hedgehog receptor Patched regulates both localization and turnover. *Genes Dev*. 2006; 20(18):2539–2551. [PubMed: 16980583]
25. Herrmann JL, Briones F Jr, Brisbay S, et al. Prostate carcinoma cell death resulting from inhibition of proteasome activity is independent of functional Bcl-2 and p53. *Oncogene*. 1998; 17(22):2889–2899. [PubMed: 9879995]
26. Hideshima T, Richardson P, Chauhan D, et al. The proteasome inhibitor PS-341 inhibits growth, induces apoptosis, and overcomes drug resistance in human multiple myeloma cells. *Cancer Res*. 2001; 61(7):3071–3076. [PubMed: 11306489]
27. Yin D, Zhou H, Kumagai T, et al. Proteasome inhibitor PS-341 causes cell growth arrest and apoptosis in human glioblastoma multiforme (GBM). *Oncogene*. 2005; 24(3):344–354. [PubMed: 15531918]
28. Goodrich LV, Johnson RL, Milenkovic L, et al. Conservation of the hedgehog/patched signaling pathway from flies to mice: induction of a mouse patched gene by Hedgehog. *Genes Dev*. 1996; 10(3):301–312. [PubMed: 8595881]

29. Chauhan D, Hideshima T, Mitsiades C, et al. Proteasome inhibitor therapy in multiple myeloma. *Mol Cancer Ther.* 2005; 4(4):686–692. [PubMed: 15827343]
30. Lauth M, Bergstrom A, Shimokawa T, et al. Inhibition of GLI-mediated transcription and tumor cell growth by small-molecule antagonists. *Proc Natl Acad Sci U S A.* 2007; 104(20):8455–8460. [PubMed: 17494766]
31. Sanchez P, Ruiz i Altaba A. In vivo inhibition of endogenous brain tumors through systemic interference of Hedgehog signaling in mice. *Mech Dev.* 2005; 122(2):223–230. [PubMed: 15652709]
32. Ellis T, Smyth I, Riley E, et al. Patched 1 conditional null allele in mice. *Genesis.* 2003; 36(3): 158–161. [PubMed: 12872247]
33. Uhmann A, Dittmann K, Nitzki F, et al. The Hedgehog receptor Patched controls lymphoid lineage commitment. *Blood.* 2007; 110(6):1814–1823. [PubMed: 17536012]
34. Mak KK, Chen MH, Day TF, et al. Wnt/beta-catenin signaling interacts differentially with Ihh signaling in controlling endochondral bone and synovial joint formation. *Development.* 2006; 133(18):3695–3707. [PubMed: 16936073]
35. Yang ZJ, Ellis T, Markant SL, et al. Medulloblastoma can be initiated by deletion of Patched in lineage-restricted progenitors or stem cells. *Cancer Cell.* 2008; 14(2):135–145. [PubMed: 18691548]
36. Zurawel RH, Allen C, Chiappa S, et al. Analysis of PTCH/SMO/SHH pathway genes in medulloblastoma. *Genes Chromosomes Cancer.* 2000; 27(1):44–51. [PubMed: 10564585]
37. Mao J, Ligon KL, Rakhlin EY, et al. A novel somatic mouse model to survey tumorigenic potential applied to the Hedgehog pathway. *Cancer Res.* 2006; 66(20):10171–10178. [PubMed: 17047082]
38. Rajkumar SV, Richardson PG, Hideshima T, et al. Proteasome inhibition as a novel therapeutic target in human cancer. *J Clin Oncol.* 2005; 23(3):630–639. [PubMed: 15659509]
39. Hemeryck A, Geerts R, Monbaliu J, et al. Tissue distribution and depletion kinetics of bortezomib and bortezomib-related radioactivity in male rats after single and repeated intravenous injection of ¹⁴C-bortezomib. *Cancer Chemother Pharmacol.* 2007; 60(6):777–787. [PubMed: 17285316]

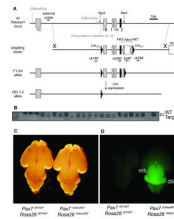


Fig. 1.

Mouse lines were generated for a conditional medulloblastoma model. **(A)** For the *Ptc1* conditional mouse line, a targeting vector was designed for which exons 1B, 1, 1A and 2 were flanked by Lox511 sites at the locations of *KpnI* and *SacI* restriction endonuclease sites. This *F1-2p* allele (not shown) contains the *neomycin resistance gene* (*Neo* positive), whereas the *F1-2m* allele has had the FRT-flanked *neomycin resistance gene* removed by Flpe (*Neo* minus). In the presence of Cre, the inactivated *DELI-2* allele is generated. The positions of PCR genotyping primers ck192, ck295, ck296 and ba97 are shown. **(B)** Southern hybridization of ES cell clones using an external probe demonstrates an 8.2 kB downshift for multiple samples that harbor the *Ptc1* targeted conditional modification. **(C and D)** We have previously described generation of the *Pax7^{ICNm}* mouse and its myogenic expression. Shown here is the central nervous system lineage of *Pax7* in neonates. For mice doubly heterozygous for the *Pax7^{ICNm}* allele and an *eYFP* reporter allele, the *Pax7* lineage includes both the midbrain (mb) and the cerebellum (cbl).

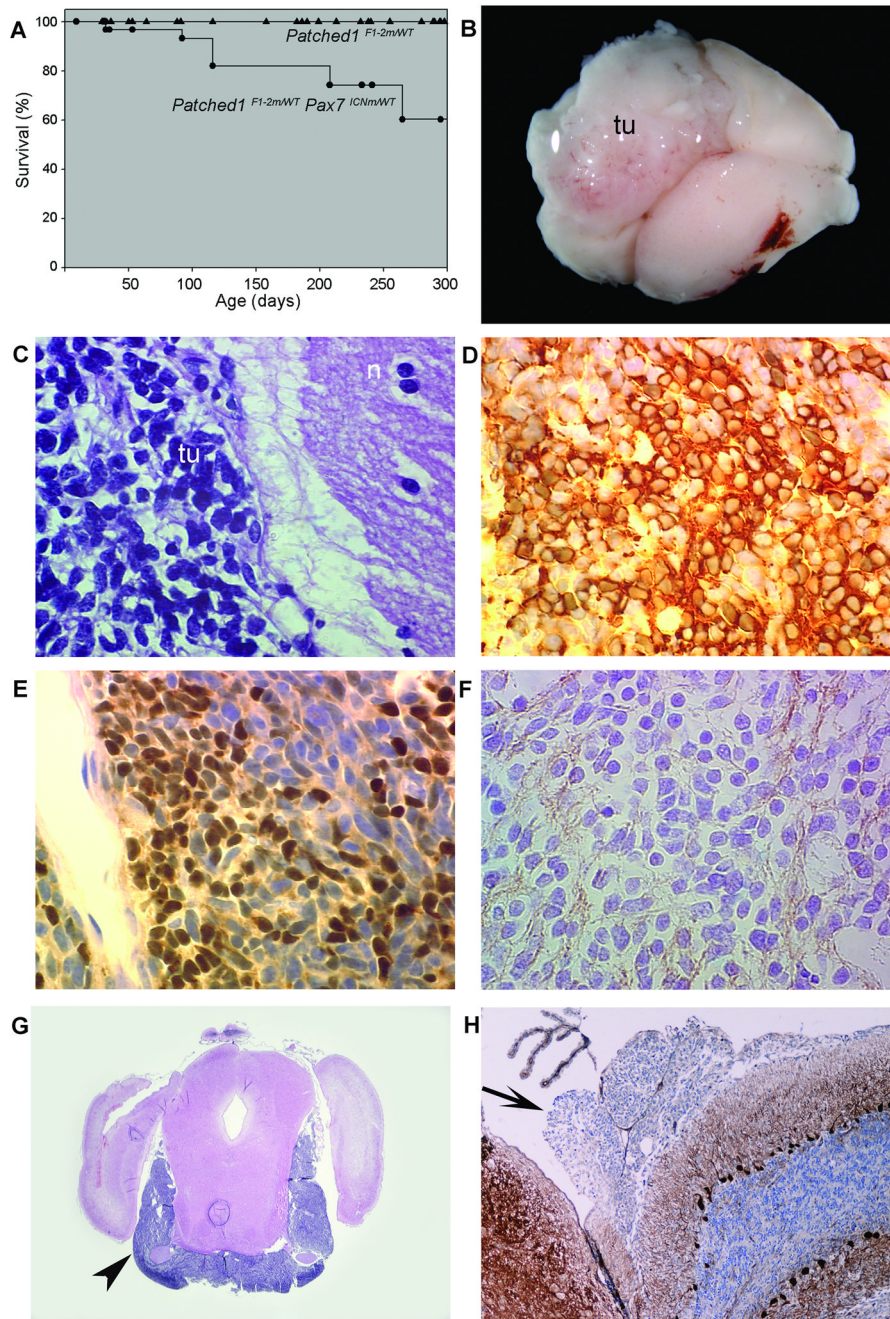


Fig. 2. A Conditional model of classic medulloblastoma with leptomenigeal metastases was established. (A) Significant difference in survival for *Pax7^{ICNm/WT} Ptc1^{F1-2m/WT}* (●) experimental mice, and *Ptc1^{F1-2m/WT}* (▲) control mice, $p = 0.0002$. The cause of death in *Pax7^{ICNm/WT} Ptc1^{F1-2m/WT}* mice was exclusively brain tumors. (B) Gross inspection of the brain from the mouse in shows a large left cerebellar tumor mass (tu). (C) Histology shows tumor cells (tu) adjacent to normal neuropil (n). Tumors were immunoreactive for medulloblastoma markers β -Tubulin (D), NeuN (E), and synaptophysin (F). (G) Coronal hematoxylin and eosin section reveals evidence of extensive leptomenigeal metastases (arrowhead). (H) Immunohistochemistry demonstrating a focus of metastasis by

leptomeningeal spread (arrow) to the fourth ventricle, weakly immunoreactive for Calbindin.

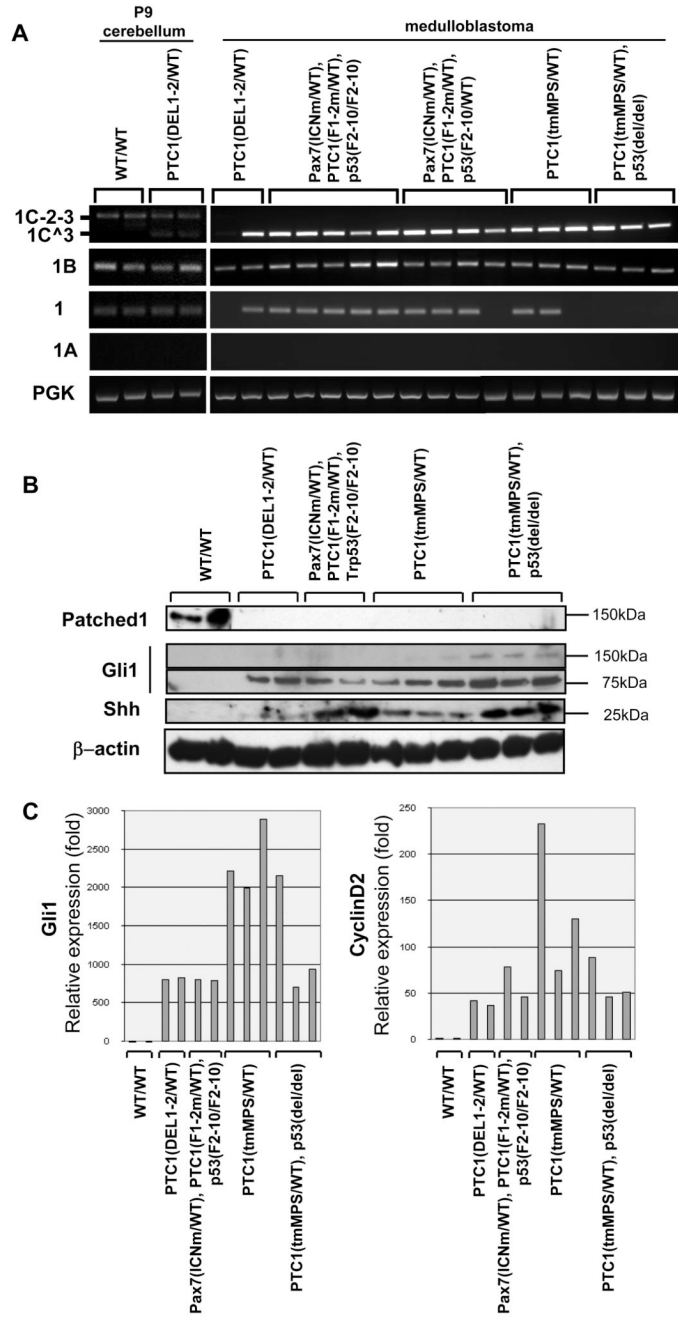


Fig. 3. *Ptc1* splice variants are present, but *Ptc1* protein product is completely absent from tumors. (A) Expression of the alternative *Ptc1* splice variants in primary tumors. Medulloblastoma tumors were taken from mice derived from our conditional allele, *Ptc1*^{F1-2m/WT} or *Ptc1*^{DEL1-2}, or from a germline model, *Ptc1*^{tmMPS/WT}. Some mice carried a conditional allele of *p53*, *p53*^{F2-10}, or a germline allele of *p53*, *p53*^{del}. Postnatal day 9 (P9) wild type mouse brain was used as a control. The *1B* transcript variant is expressed in all tumors tested. Exon 1A and 12b splice variants are not detected in tumors, whereas the exon 1 variant is variable expressed across models. (B) Immunoblotting of *Ptc1*, *Gli1* and *Shh*. Full length *Ptc1* protein (approximately 145 kDa) is detected in the control postnatal brain tissue,

but no Ptc1 isoform is detected in any medulloblastoma sample for the genotypes tested. The 75 kDa form of Gli-1 is detected in all tumors. The cleavage form of Shh was much more highly expressed in tumors with *p53* mutations. (C) Quantitative RT-PCR demonstrates dramatic over-expression of Shh target genes, *Gli1* and *CyclinD2*, by 100 – 1000 fold in all models of medulloblastoma.

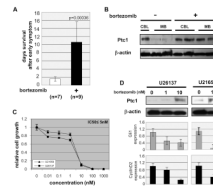


Fig. 4.

In vivo and *in vitro* effect of bortezomib in medulloblastoma. **(A)** Survival of bortezomib-treated mice. Medulloblastoma-bearing mice were administered with DMSO (n=7) or bortezomib (1mg/kg, n=9) at the earliest sign of disease (ataxia). **(B)** Immunoblotting of Ptc1. Full length Ptc1 protein is restored after treatment with bortezomib (1mg/kg, once a week by intraperitoneal injection) in medulloblastoma-bearing mice. wt CBL; wildtype cerebellum, MB; medulloblastoma. **(C)** *in vitro* cell growth assay of bortezomib in primary cultured mouse medulloblastoma cell lines (U21659 and U26137). IC₅₀ ≤ 5nM. **(D)** Immunoblotting of Ptc1. Ptc1 protein is accumulated in dose-dependent manner of bortezomib in murine medulloblastoma cell lines. (bottom) Quantitative RT-PCR demonstrates dose-dependent decrease of *Gli1* and *CyclinD2* transcription following treatment with bortezomib.

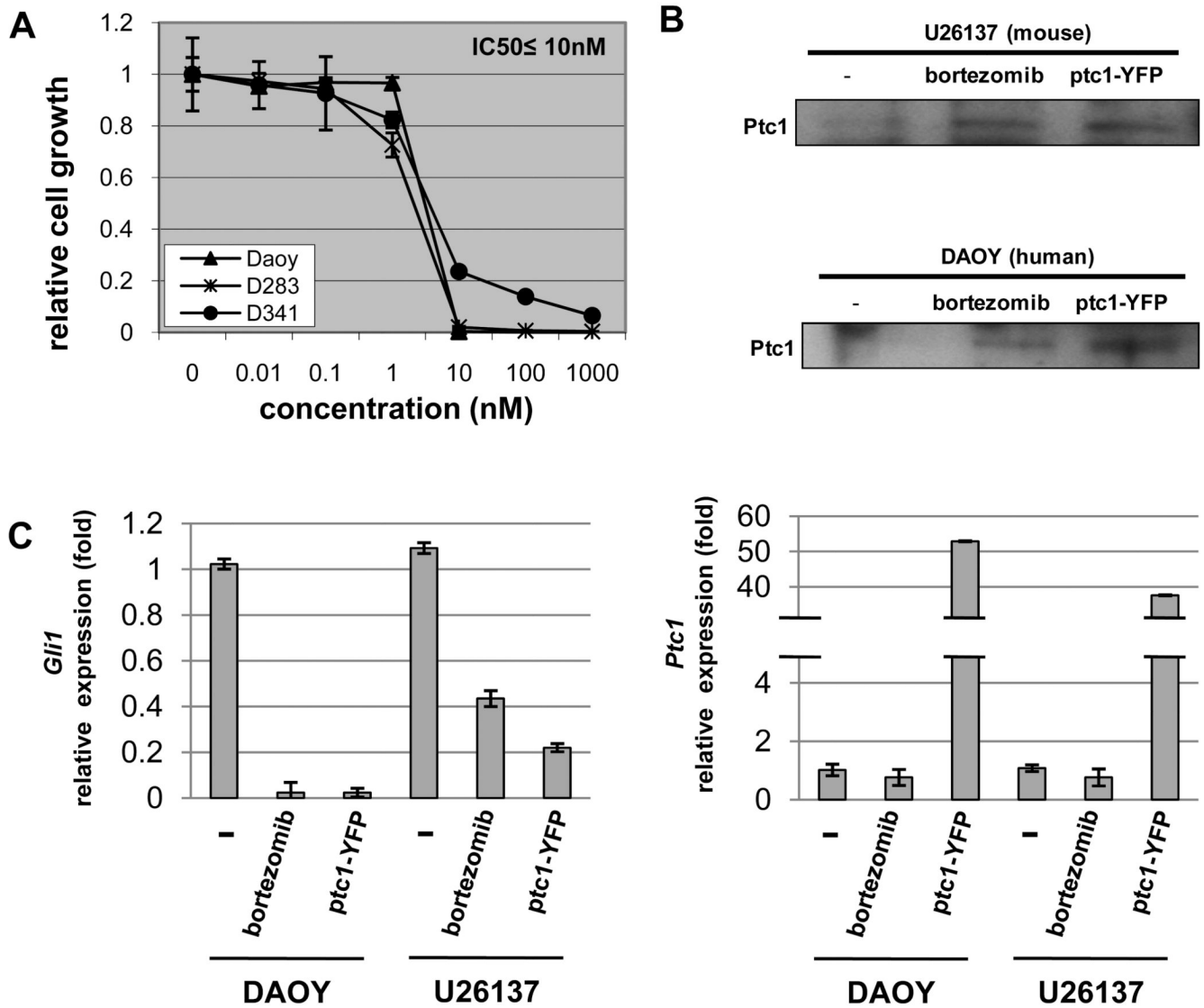


Fig. 5. Bortezomib restores Ptc1 and dampens Shh overdrive in human as well as mouse medulloblastoma cell lines. **(A)** *in vitro* cell growth assay of bortezomib in human medulloblastoma cell lines (DAOY, D283 and D341). IC₅₀ ≤ 10nM. **(B)** Accumulation of Ptc1 protein (IP-Western) after treatment of bortezomib or transient transfection of Ptc1-YFP in both human (DAOY) and mouse (U26137) medulloblastoma cell lines. **(C)** Decrease of *Gli1* transcription is accompanied with Ptc1 protein accumulation by either treatment of bortezomib (10 nM) or transfection of Ptc1-YFP in both human and mouse medulloblastoma cell lines. *Ptc1* transcription is suppressed with treatment of bortezomib, while Ptc1-YFP transfected cell lines show redundant *Ptc1* transcription.